

## **LAKE NUBIA BATHYMETRY DETECTION BY SATELLITE REMOTE SENSING**

*M. A. Elsayhaby<sup>1</sup>, O. Makboul<sup>2</sup>, and A. M. Negm<sup>3</sup>*

<sup>1</sup> *Civil Engineering Department, Faculty of Engineering, Aswan University, Aswan, 81542, Egypt,  
E-mail: moh\_78\_78@yahoo.com, mohamed.sahabi@aswu.edu.eg*

<sup>2</sup> *Arab Academy for Science, Technology and Maritime Transport, Alexandria-21913, Egypt,  
E-mail: omarm526@gmail.com*

<sup>3</sup> *Department Water and Water Engineering Dept., Faculty of Engineering, Zagazig University,  
Zagazig, 44519, Egypt, E mail: amnegm85@yahoo.com, amnegm@zu.edu.eg*

### **ABSTRACT**

Optical remote sensing offers an alternative to traditional hydrographic surveys for measuring water depth, with the advantage that data are collected synoptically over large areas. By comparison with the traditional method, remote sensing can produce more flexible, efficient and cost effective means of mapping bathymetry. There are several factors affected when measuring depth in shallow water especially rivers such as the degree of transparency of the water, water turbidity, nature of the bottom and the reflection from surrounding area. This research was conducted on the Aswan High Dam Lake (AHDL) (particularly Nubia Lake) using Landsat-8 multi-spectral bands with resolution 30m. Reflectance from multiband bands combination were used to improve the results of bathymetric information extraction and calibrated with in-situ measurements. This method is based on using Multiple Linear Regression (MLR) using logarithms of reflectance bands. We also quantified the error between in-situ measurements and satellite estimated lake depth values. Our results indicated a good correlation ( $R= 0.5$ ) and Root Mean Square Error (RMSE= 0.6m) for testing data set. Finally, the computed depths from the satellite remote sensing data were used to estimate the storage capacity of Lake Nubia (LN). The present computations are compared by the method of cross sections that was adopted by Aswan High Dam Authority (AHDA) and Nile Research Institute (NRI) to detect the storage capacity of LN through the investigated field trips.

**Keywords:** Remote Sensing, Lake Nubia, Multiply Linear Regression, Satellite derived bathymetry

### **1 INTRODUCTION**

Accurate bathymetric measurements are considered of fundamental importance towards monitoring sea bottom, producing nautical charts and coastal and marine planning and management, Raj & Sabu (2013). Recently, bathymetric surveying of shallow water has been mainly based on conventional ship-borne echo sounding operations. However, this technique demands cost and time, particularly in shallow waters, where a dense network of measured points is required, Pattanaik et al. (2015). Single Beam Echo Sounder (SBES) on survey vessel can acquire single point depths along sparsely surveying scan lines up to 500 m depths. Multi-beam echo sounder (MBES) improves the scanning with wide swath coverage below the vessel scan line resulting better resolution of the resulting sounding, Su et al. (2008) with full bottom coverage and depth accuracy up to 1cm.

Since the late 1970s it has been perceived that, as an alternative to discussed active remote detecting devices (sonar and LIDAR), shallow-water depth can likewise be assessed utilizing multi-band satellite symbolism and latent passive remote sensing detecting procedures Lyzenga (1981) and Philpot (1989). This method has a lower precision, lower cost, short-period and wide coverage. The theory behind all bathymetric mapping using optical remote sensing is that different wavelengths of light penetrate water with varying degrees. When the light passes through water, it becomes attenuated by interaction with water column according to Beers law, (Ehses & Rooney (2015) and Green et al. (2000)). Therefore, the light is reflected from the seabed in shallow water which appears bright as a less amount of light has been absorbed. Conversely, deep areas appear darker, Melsheimer & Chin

(2001). All the radiance and irradiances are decreased approximately exponentially with depth, Stumpf et al. (2003).

Optical Remote Sensing (RS) can be implemented for bathymetry derivation by using two methods: analytical modeling and empirical modeling, Gao (2009). Analytical modeling of bathymetry is based on the propagation of light in water. For the establishment of this model, a number of optical properties of water such as the attenuation coefficient and backscattering are required as inputs, Jawak & Luis (2016). In empirical modeling, the relationship between the remotely sensed radiance or reflectance of a water body and the depth at sampled locations are established empirically without consideration to how the light is transmitted in water, Doxani et al. (2012). Lyzenga developed the first empirical methods for estimating bathymetry based on Lambert–Beer law of attenuation, Lyzenga (1978), than the satellite has experienced significant evolution in both spatial and spectral resolutions. Lyzenga (1985) developed a technique to derived bathymetry by using A log-linear relationship between corrected image reflectance values and water depths after removing the sun-glint and water column effect by subtracting the minimum spectral radiance of deep water area from bands, Lyzenga (1981). Stumpf et al. (2003) developed a technique depending on the ratio of different attenuation rates between wavebands to determine depth. The band with a higher absorption rate will decrease proportionally faster than the band with a lower absorption rate. The change in the ratio between the bands will affect the higher absorption band more with increasing depth therefore, as depth increases the change in ratio between the two bands will be affected more by depth. Although this theory does not have sound physical foundation and needs pre coefficients selected with trial and error by the user. Some researchers try to derive bathymetry using empirical modeling such as Ceyhun & Yalçın (2010) used Artificial Neural Network (ANN) to derive bathymetric maps in shallow waters via remote sensing images and sample depth measurements. Corucci (2011) used neuro-fuzzy technique applied to two Quick bird images of the same area, acquired in different years and meteorological conditions. Su et al. (2008) tried to calibrate the parameters for the non-linear inversion model proposed by Stumpf automatically using the Levenberg-Marquardt optimization algorithm.

The accuracy of the retrieved bathymetry from water depends on several limitations and is called practical limitations, Green et al. (1996). Practical limitations arising from sensor specifications such as Turbidity and variations in water color may confuse bathymetry, remote sensing which generally provides geomorphologic rather than biological information, disparity between dates of image and field work complicates image interpretation and spatial and spectral resolution which are too coarse Green et al. (2000). Water turbidity is the important factor affecting the accuracy; as it obstructs the path of Electromagnetic Radiation (EMR). Reflectance from suspended particles becomes confused with bottom reflectance. Water of different turbidity levels scatters the incoming radiation differently Gao (2009). The total signal received at the satellite altitude is dominated by reflectance contributed through atmospheric scattering processes. Therefore, it is advisable to correct for atmospheric effects to retrieve any quantitative information for surface from the image, Mishra et al. (2005).

The objective of this research is to propose a methodology for bathymetry detection of Lake Nubia using Landsat-8 multiband combination after removing atmosphere and sun glint effects and their logarithms as the dependent variable and in-situ measurement as the independent variable in Multiply Linear Regression (MLR). The water quality status of Lake Nubia ranges from excellent (according to the Egyptian water quality standards for surface fresh waterways) to good.

## 2 MATERIALS AND METHODS

### 2.1 The study area

AHDL is one of the greatest man-made Lakes in the world, created after the construction of the Aswan High Dam (AHD). This Lake extends for 500 km along the Nile River from the southern part of Egypt to the northern part of Sudan. It covers an area of about 6,000 km<sup>2</sup>, of which two-thirds (known as Lake Nasser, 350 km) is in Egypt and one-third (called Lake Nubia, 150 km) is in Sudan, Negm et al. (2017) as shown in Figure 1.

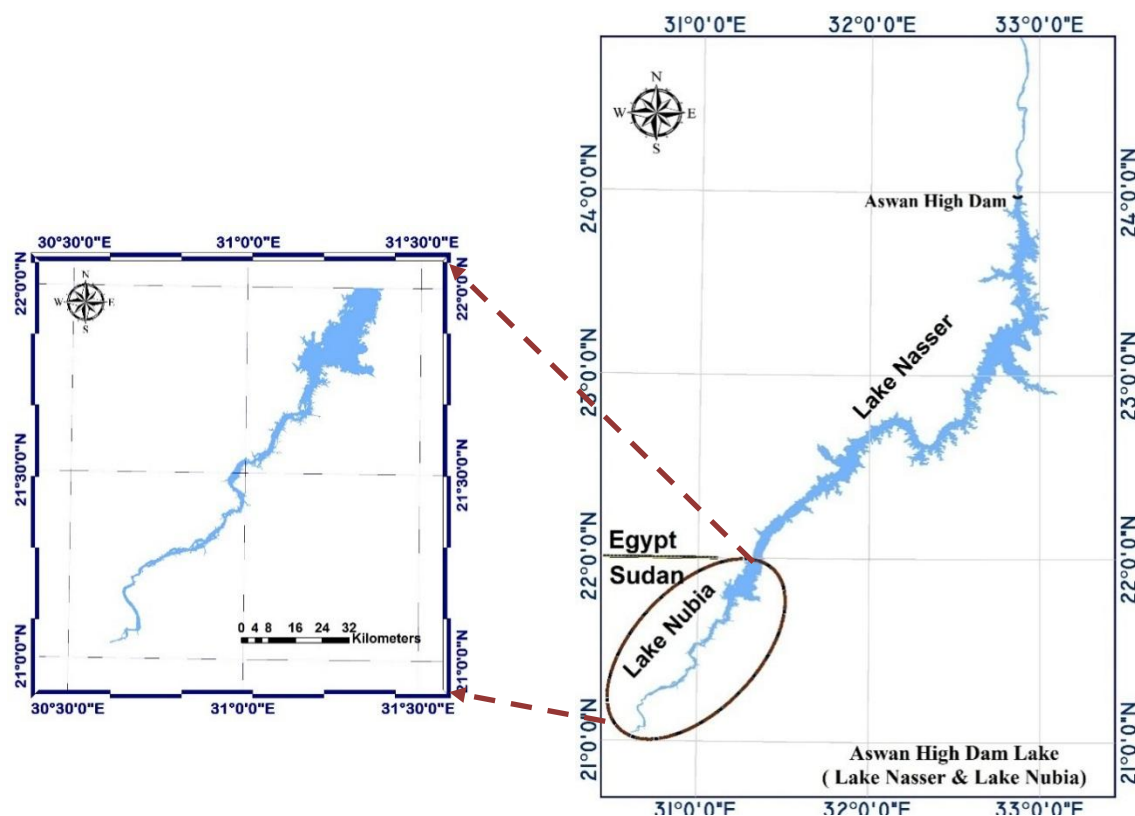


Figure 1. Location map of the study area within Aswan High Dam Lake.

Lake Nubia, the study area in this paper, is located between latitudes 21° 02' 00" and 22° 00' 00" N (upstream the AHD). The southern two thirds of this Lake are narrow, while the remaining northern part is much wider as indicated in Figure 1.

## 2.2 Hydrographic survey data

The hydrographic survey data presented by Easting, Northing, and Elevation (E, N, and Z) were used to describe the geometry of Lake Nasser study area for year 2012. These data were conducted by (AHDA and NRI) using the Odom Hydrographic echo-sounder device (Hydrotrac II) with accuracy up to  $0.01\text{m} \pm 0.1\%$  of the measured depth.

## 2.3 Sensor data

Landsat-8 collects image data in 11 spectral bands with a 30 m spatial resolution with (Path/Row = 175/045). The bands used for detecting bathymetry in this study are coastal/ aerosol (0.435-0.451  $\mu\text{m}$ ), blue (0.452-0.512  $\mu\text{m}$ ), green (0.533-0.590  $\mu\text{m}$ ), red (0.636-0.673  $\mu\text{m}$ ) and Near Infrared (NIR) (0.851-0.879  $\mu\text{m}$ ), USGS (2015). The Landsat-8 data used in this study are collected on 24-05-2013 with an average cloud cover less than 10%. The data were downloaded freely from the earth explorer USGS in level 1 Geotiff (systematic correction) product. These images were geo-referenced by USGS using the world reference system (WGS-84 datum) to Universal Transverse Mercator system (UTM) zone, 36 North projections.

## 3 METHODOLOGY

### 3.1 Imagery data pre-processing

Satellite images are affected by a variety of environmental factors such as atmosphere and sun specular. It needs pre-corrections to avoid the influence of the inversion depth. The pre-processing has

great effect on improving the precision of inversion depth. The radiometric corrected pixel values are firstly converted to spectral reflectance. Second, two steps corrections are applied to the image; atmospheric correction and Sun-glint correction. The sequence of applying these two corrections is arbitrary. Some researchers started with atmospheric correction followed by sun-glint correction while others reverse this procedure, Mohamed et al. (2016). Model parameters are obtained as a result of training and testing processes. The methodology is summarized according to flow chart in Figure2. The image is first filtered to discard the atmospheric. Secondly, water reflectance values were isolated from the land. Thirdly, sun specular effect was removed to decrease noise and scattering effects on the input image. The reflectance values corresponding to the point, where there are available depth measurements, are extracted from multispectral images for usage bands.

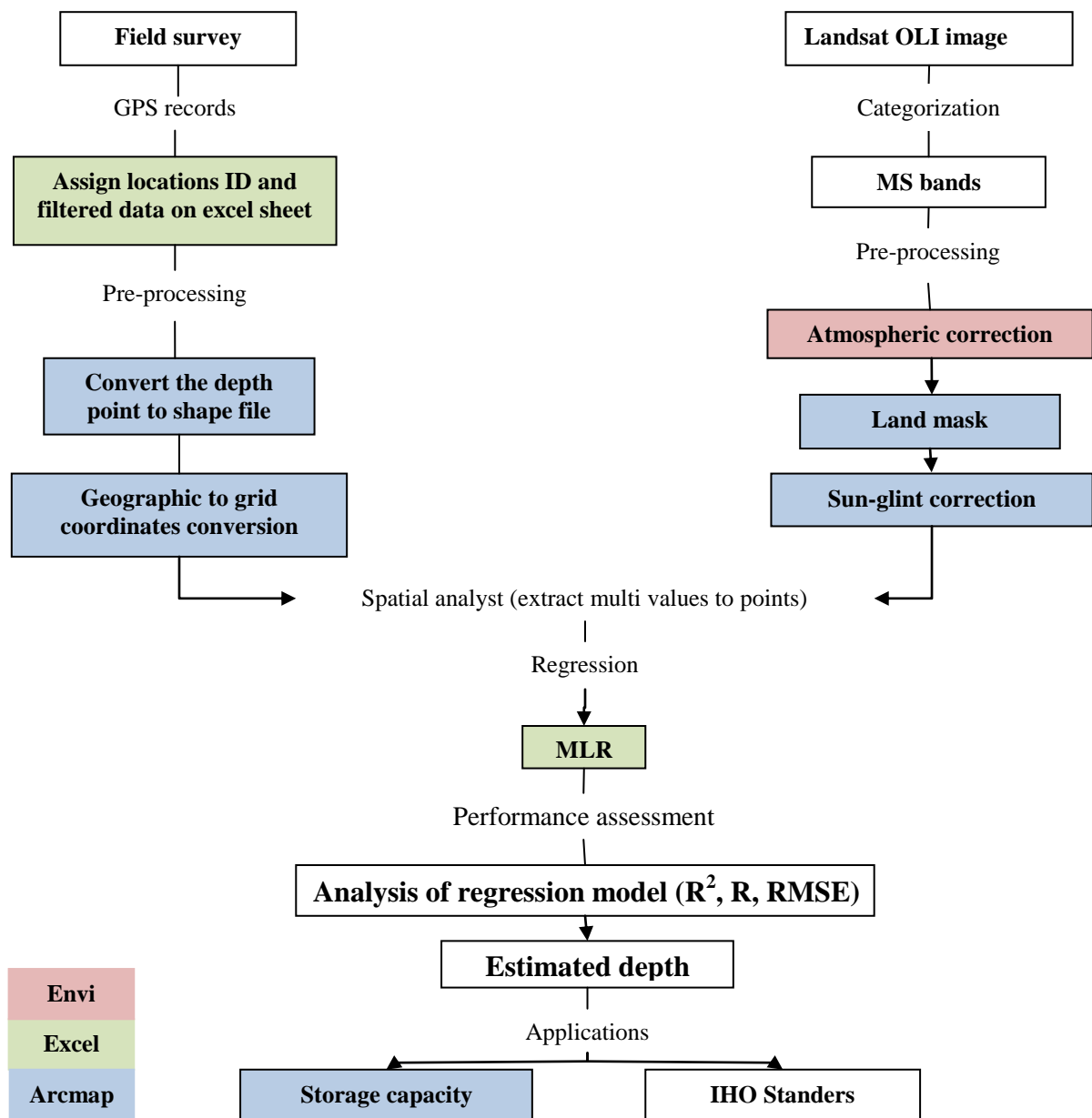


Figure 2. Flowchart showing methodology adopted in this study to estimate the depth.

### 3.2 Converting to radiance

Convert the digital number (DN) to the spectral radiance at the aperture ( $L_\lambda$ ) is measured in (watts/ meter squared \* ster \*  $\mu\text{m}$ ) using the gain and bias information of sensor bands as follows Equation 1.

$$L_\lambda = ML * Q_{cal} + AL \quad (1)$$

Where, ML is Band-specific multiplicative rescaling factor (RADIANCE\_MULT\_BAND\_x) or Rescaling gain factor (Gain) from Land-sat metadata files,  $Q_{cal}$  is calibrated standard product pixel values (DN) and AL is Band-specific additive rescaling factor (RADIANCE\_ADD\_BAND\_x) or Rescaling bias factor (Bias) from Land-sat metadata file, Chander et al. (2009).

### 3.3 Applying atmospheric correction

The solar radiation passes through the atmosphere before collected by the sensor. Therefore images are affected by several factors such as water vapor and distribution of aerosols (visibility). In this paper, the FLASSH model in ENVI software is used to correct the atmospheric effect that applied to the solar wavelength. FLAASH normally retrieves aerosol and water vapor information from the image, providing well-adjusted input for the atmospheric correction. FLAASH starts from a standard equation for spectral radiance at a sensor pixel according to Equation 2, ENVI (2009).

$$L = \left( \frac{A\rho}{1-\rho_e^s} \right) + \left( \frac{B\rho_e}{1-\rho_e^s} \right) + L_a \quad (2)$$

Where,  $\rho$  is the Pixel surface reflectance,  $\rho_e$  is an average surface reflectance for the pixel and a surrounding region,  $s$  is the spherical albedo of the atmosphere and  $L_a$  is the radiance back scattered by the atmosphere. A and B are coefficients that depend on atmospheric and geometric conditions but not on the surface. Moreover, A, B, S and  $L_a$  are depending on water vapor amount. The input files must contain calibrated radiance values and converted to BSQ or BIP format before the atmospheric correction. In addition to the image file to be corrected, FLAASH also needs information on the geographical centre location of the image and the time it was captured. This information can't be retrieved automatically from the data file, but must be entered by the user. An atmospheric model must be selected depending on climate (latitude and time of year). Urban aerosol model is selected depending on the expected type of aerosols and visibility present.

### 3.4 Land masking

When extracting aquatic information, it is useful to eliminate all upland and terrestrial features. Thus, all upland features were masked out of the image. The "land-mask" restricts the spectral range to aquatic features and allows for detailed feature discrimination. Reflectance values of the NIR band were used to prepare the mask which was subsequently applied to all the bands, Mishra et al. (2005). The threshold value for land/water was calculated to separate water area.

### 3.5 Applying sun glint correction

Specular reflection of solar radiation, known as sun glint must be removed for accurate benthic habitat classification. Hochberg provided a method to remove sun glint by using the brightness of near-infrared NIR band, Hochberg et al. (2003). Hedley proposed revised method depending on Hochberg assumption that based on the linear relationship between NIR and visible bands using linear regression, Hedley et al. (2005). By using linear regression of NIR brightness (x-axis) against the visible band brightness (y-axis), this would be homogeneous if not for the presence of sun glint (deep water). The slope of the regression is then used to predict the brightness in the visible band by using Equation 3. The minimum sample size required is two pixels.

$$R'_i = R_i - b_i(R_{NIR} - MIN_{NIR}) \quad (3)$$

Where  $R'_i$  is the sun-glint corrected pixel brightness in band  $i$ ,  $b_i$  is the product of regression slope,  $R_{NIR}$  is corresponding pixel value in NIR band and  $MIN_{NIR}$  is the min NIR value existing in the sample.

### 3.6 Statistical models

#### 3.6.1 Multiple linear regressions

Multiple linear regression attempts to model the relationship between two or more explanatory variables and a response variable by fitting a linear equation to observed data. Every value of the independent variable  $x$  is associated with a value of the dependent variable  $y$ . The regression line for explanatory variables is defined to be as Equation 4.

$$y = \alpha + \beta_1 X_1 + \beta_2 X_2 + \dots + \beta_n X_n \tag{4}$$

Where,  $\alpha$  is called the intercept,  $\beta_i$  is called slopes or coefficients and  $X_n$  is the reflectance of spectral bands. The main objective in using this technique is to predict the variability the dependent variable based on its covariance with all the independent variables.

## 4 RESULTS

Model parameters are obtained as a result of training and testing processes. The image is first filtered to discard the atmospheric and sun specular effect to decrease noise and scattering effects on the input image. After that the reflectance values corresponding to the point where there are available depth measurements are extracted from multispectral images for usage bands. The input reflectance and in-situ measurement are separated into two parts as training (70%) and testing (30%) data sets for MLR. Once the model inputs are prepared, model architecture and parameters can be readily determined.

Multiple linear regression analysis (MLR) was carried out in Microsoft Excel 2007 to calculate the coefficient of regression models as the following Equation (5).

$$Z = -47.73 + 2.37 * L_C + 5.67 * L_B + 2.15 * L_G + 1.25 * L_R \tag{5}$$

Where,  $L_C$ ,  $L_B$ ,  $L_G$  and  $L_R$  are respectively, the logarithms of the reflectance of coastal, blue, green and red bands. The coefficient of determination  $R^2$  and RMSE was calculated to evaluate the model as shown in Table 1. The MLR The fitted continuous model showed in Figure 3.

**Table 1. Depth estimation performance using MLR.**

| Bands      | R     |       | R <sup>2</sup> |       | RMSE  |       |
|------------|-------|-------|----------------|-------|-------|-------|
|            | Train | Test  | Train          | Test  | Train | Test  |
| 1, 2, 3, 4 | 0.424 | 0.500 | 0.180          | 0.250 | 1.783 | 0.605 |

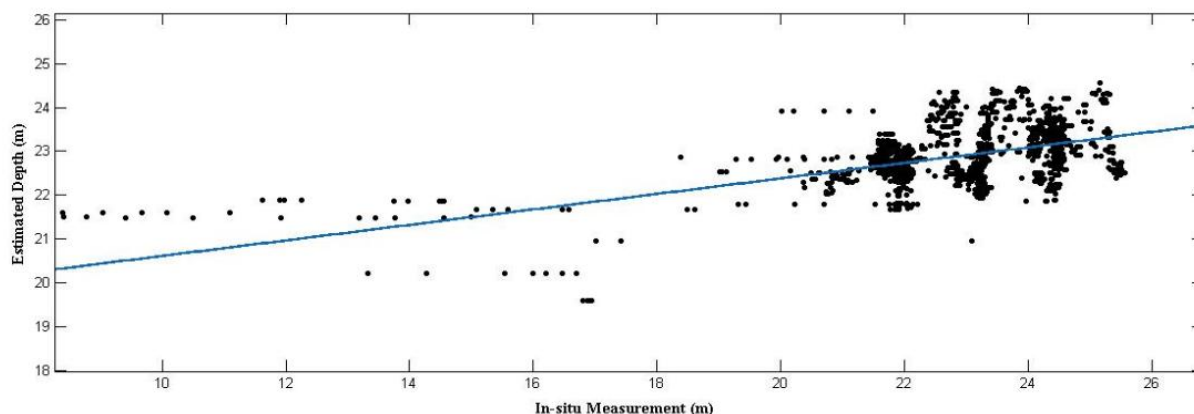


**Figure 3. MLR continuous fitted model. Depths are represented as points.**

## 5 DISCUSSION AND APPLICATION

Our results show that the multiple regression method has better performance in terms of the correlation coefficient (R) and root mean square error (RMSE) are 0.50 and 0.61m for testing data set. However for training data set, the MLR has lower performance regarding both R and RMSE. On the other hand, the observation are supported by the data scattering presented in Figure 3 shows that the MLR has good predicting to the depth from 20m to 25m and lower predicting to the depth from 8m to 20m. This could be explained by Landsat-8 has lower resolution 30m×30m and fewer pixels therefore there is no possibility to estimate water depths for regions smaller than 900m<sup>2</sup>. Also, the depth ratio which ranges from 8m to 20m relatively to the available in-situ measurements is 4.4%. Differences in the bottom type misleading the results since the bottom type in the study area are silt, mud and sand.

Estimating bathymetric data provides many applications which aid in the management of lakes. One of these applications to be applied (involved) in this study is to estimate the storage capacity of LN which is essential for the managers and decision makers of water management sector for both Egypt and Sudan countries. Two methods were used in the current study to estimate the water capacity of LN. The first method is estimating the storage capacity via building 3D profile of the lake (the present approach). The second one is the storage capacity estimation approach using the complementary cross sections method adopted by AHDA and NRI (the traditional method). The reference method is the traditional method.

The present approach of estimating the lake storage capacity rely upon using the satellite estimated lake depths to establish the 3D profile of the lake utilizing ArcGIS software.

The created 3D bed surface profile of the study area from the estimated satellite lake depths is shown in Figure 4. For more details about building the 3D profile of Lake Nubia, interested readers can consult Negm & Elsayabi (2016).

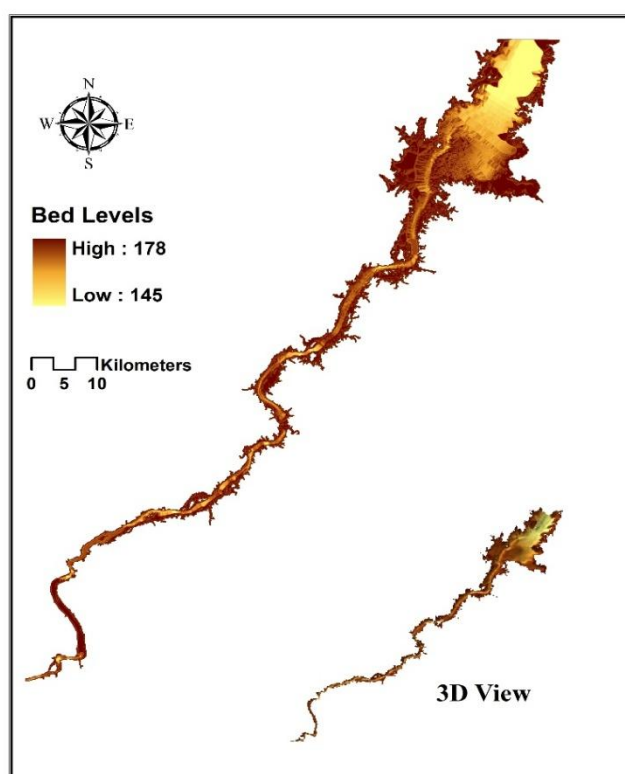


Figure 4. The generated bed surface of Lake Nubia based on the estimated satellite lake depths.

Table 2 illustrates that the computed storage capacity of LN for year 2012 by the present approach was about  $3.82 \times 10^9$  m<sup>3</sup> at water level 175 m amsl and the estimated storage capacity by AHDA (the

traditional method) was equal to  $4.05 \times 10^9 \text{ m}^3$  at the same water level in the same year, NRI (2012). This means that the computed storage capacity by the present approach is somewhat lower than the results of the traditional method.

**Table 2. Comparison of results between the present approach and the traditional method for estimating the storage capacity of Lake Nubia.**

| year | Storage capacity by the present approach ( $\text{m}^3$ ) | Storage capacity by traditional method ( $\text{m}^3$ ) |
|------|---|---|
| 2012 | $3.82 \times 10^9$  | $4.05 \times 10^9$                                      |

It could be concluded that the present approach underestimates the storage capacity by about 5.68% compared to the results of the traditional method. Accordingly, the estimated bathymetric data by the applied approach in the present study can be used to estimate the storage capacity of LN instead of the costly field measurements.

It is worth to compare the results with International Hydrographic Organization Standard (IHOs). The maximum allowable Total Vertical Uncertainty (TVU) for reduced depths specifies the uncertainty to be achieved to meet each order of survey. In Minimum Standards for Hydrographic Surveys special order for areas where under keel clearance is critical according to Equation 6.

$$TVU = \pm \sqrt{a^2 + (b * d)^2} \quad (6)$$

Where a is represents that portion of the uncertainty that does not vary with depth, b is a coefficient which represents that portion of the uncertainty that varies with depth, d is depth of water and b x d represents that portion of the uncertainty that varies with depth. We found that TVU using satellite derived bathymetry method is  $\pm 0.301\text{m}$  since  $a = 0.25$  and  $b = 0.0075$  and  $d = 22.5$  which represent the average depth in the study area.

## 6 CONCLUSION

In this research, the proposed methodology used bands corrected from atmospheric and sun-glitter errors which influence the bathymetry and their logarithms as input values. The used approaches were tested by data collected using Echo-Sounder for measuring water depths. Results showed that the errors around 1.7m can be obtained. This accuracy may be enough when using bathymetry by remote sensing in the preliminary survey. Moreover, the results indicated that the computed storage capacity of LN for the year 2012 at water level 175 m amsl, based on the generated 3D profile of the lake from the satellite estimated lake depths (present approach), is about  $3.82 \times 10^9 \text{ m}^3$ . Also, the results illustrated that the present approach underestimated the storage capacity of the lake by less than 6% compared to the results of the method used by AHDA, based on the complementary cross sections for the year 2012 at the same water level (175 m amsl).

## ACKNOWLEDGMENTS

Aswan High Dam Authority (AHDA) and the Nile Research Institute (NRI) are hereby acknowledged for providing the facilities utilized during this research work.

## ABBREVIATIONS

The following abbreviations were used in this study

- AHD Aswan high dam
- AHDA Aswan high dam authority
- AHDL Aswan high dam lake
- amsl above mean sea level



EMR Electromagnetic radiation  
 IHO International hydrographic organization  
 LN Lake nubia  
 NRI Nile research institute  
 RMSE Root mean square error  
 RS Remote sensing  
 TVU Total vertical ucertainty

## REFERENCES

- Ceyhun, Ö. and Yalçın, A. (2010) *Remote sensing of water depths in shallow waters via artificial neural networks*, Estuarine, Coastal and Shelf Science, 89(1), pp.89–96.
- Chander, G. Markham, B, L and Helder, D, L. (2009) *Remote Sensing of Environment Summary of current radiometric calibration coefficients for Landsat MSS, TM, ETM +, and EO-1 ALI sensors*, Remote Sensing of Environment, 113(5), pp.893–903.
- Corucci, L. (2011) *Approaching bathymetry estimation from high resolution multispectral satellite images using a neuro-fuzzy technique*, Journal of Applied Remote Sensing, 5(1), p.053515.
- Doxani, G., Papadopoulou, M., Lafazani, P., Pikridas, C. and Tsakiri-Strati, M. (2012) *Shallow-Water Bathymetry Over Variable Bottom Types Using Multispectral WorldView-2 Image*, ISPRS - International Archives of the Photogrammetry, Remote Sensing and Spatial Information Sciences, XXXIX-B8(September), pp.159–164.
- Ehse, J.S. and Rooney, J. J. (2015). *Depth Derivation Using Multispectral WorldView-2 Satellite Imagery*, Civil and Environmental Engineering, (June), U.S. Dep. Commer., NOAA Tech. Memo., NOAA-TM-NMFS-PIFSC, pp.24–46.
- ENVI, (2009). *ENVI Atmospheric Correction Module: QUAC and FLAASH User's Guide*, ITT Visual Information Solutions.
- Elsahabi, M.; Negm, A. M. (2016) *Building 3D profile for Lake Nubia, <Sudan> using RS/GIS for accurate estimation of Sediment*, 10<sup>th</sup> International Conference Interdisciplinarity in Engineering, INTER-ENG, 6-7 October 2016, Tirgu-Mures, Romania.
- Gao, J. (2009) *Bathymetric mapping by means of remote sensing: methods, accuracy and limitations*, Progress in Physical Geography, 33(1), pp.103–116.
- Green, E.P., Mumby, P. J., Edwards, A. J. and Clark, C. (1996) . *A Review of Remote Sensing for The Assessment and Management of Tropical Coastal Resources*. Coastal Management, 24(1), pp.1–40.
- Green, E.P. , Mumby, P. J., Edwards, A. J. and Claek, C. D.(2000) *Remote Senseing Handbook Tropical Coastal Management*, Coastal Management Sourcebook 3, UNESCO, Paris, X, pp. 316.
- Hedley, J.D., Harborne, a. R. and Mumby, P.J. (2005) *Simple and Robust Removal of Sun Glint for Mapping Shallow-Water Benthos*, International Journal of Remote Sensing, 26(10), pp.2107–2112.
- Hochberg, E.J., Andréfouët, S. and Tyler, M.R. (2003) *Sea surface correction of high spatial resolution ikonos images to improve bottom mapping in near-shore environments*, IEEE Transactions on Geoscience and Remote Sensing, 41(7 PART II), pp.1724–1729.
- Jawak, S.D. and Luis, A.J. (2016) *High-Resolution Multispectral Satellite Imagery for Extracting Bathymetric Information of Antarctic Shallow Lakes*, Proceeding of The International Society for Optical Engineering, (May), p.987819.

Lyzenga, D.R. (1978) *Passive remote sensing techniques for mapping water depth and bottom features*, Applied optics, 17, pp.379–383.

Lyzenga, D.R. (1981) *Remote sensing of bottom reflectance and water attenuation parameters in shallow water using aircraft and Landsat data*, International Journal of Remote Sensing, 2(1), pp.71–82.

Lyzenga, D.R., (1985) *Shallow-water bathymetry using combined lidar and passive multispectral scanner data*. International Journal of Remote Sensing, 6(1), pp.115–125.

Melsheimer, C. and Chin, L.S. (2001) *Extracting Bathymetry From Multi-Temporal SPOT Images*. Asian Conference on Remote Sensing, 58(12), pp.37–42.

Mishra, D.R., Narumalani, S., Rundquist, D. and Lawson, M. (2005) *Characterizing the Vertical Diffuse Attenuation Coefficient for Downwelling Irradiance in Coastal Waters: Implications for Water Penetration by High Resolution Satellite data*, ISPRS Journal of Photogrammetry and Remote Sensing, 60(1), pp.48–64.

Mohamed, H., Negm, A. M, Zahran, M. M. and Saavedra, O. C. (2016) *Bathymetry Determination from High Resolution Satellite Imagery Using Ensemble Learning Algorithms in Shallow Lakes : Case Study El-Burullus Lake*, International Journal of Environmental Science and Development, 7 (4), pp.295-301.

NRI (2012) Nile Research Institute. Annual report (1973-2012). National water Research Center, El-Qanater, Egypt.

Negm, A. M., Elsayhaby, M., Ali, K. (2017) *A Satellite Remote Sensing Approach to Estimate the Lifetime Span of Aswan High Dam Reservoir*, The Nile River, HdbEnvChem, DOI: 10.1007/698\_2017\_15, © Springer International Publishing AG.

Pattanaik, A., Sahu, K. and Bhutiyani, M.R.(2015) *Estimation of Shallow Water Bathymetry Using IRS-Multispectral Imagery of Odisha Coast*, India. Aquatic Procedia, 4(0), pp.173–181.

Philpot, W.D. (1989), *Bathymetric mapping with passive multispectral imagery*, Applied optics, 28(8), pp.1569–1578.

Raj, A. and Sabu, P. (2013) *Shallow Water Bathymetry Using Log-Linear Inversion Technique: a Case Study At Vizhinjam*, International Journal of Innovative Research in Science, Engineering and Technology , 2(1), pp.223–230.

Stumpf, R.P., Holderied, K. and Sinclair, M. (2003) *Determination of water depth with high-resolution satellite imagery over variable bottom types*, Limnology And Oceanography, 48(1\_part\_2), pp.547–556.

Su, H., Liu, H. and Heyman, W.D. (2008) *Automated Derivation of Bathymetric Information from Multi-Spectral Satellite Imagery Using a Non-Linear Inversion Model*, Marine Geodesy, 31(May), pp.281–298.

USGS. (2015) *Landsat 8 (L8) Data Users Handbook*, Department of interior U. S. Geological Survey.